2.38 Modeling of Aqueous Corrosion

A. Anderko
OLI Systems Inc., 108 American Road, Morris Plains, NJ 07950, USA

Abbreviations

CCT Critical crevice temperature
CR Corrosion rate
HKF Helgeson–Kirkham–Flowers equation of state
Me Metal
MSA Mean spherical approximation
NRTL Nonrandom two-liquid (equation)
Ox Oxidized form
Re Reduced form
SHE Standard hydrogen electrode
UNIFAC Universal functional activity coefficient (equation)
UNIQUAC Universal quasi-chemical (equation)

Symbols

a_i Activity of species i
A Surface area
A_{ij} Surface interaction coefficient for species i and j
b Tafel coefficient using decimal logarithms

$c_{i,b}$ Bulk molar concentration of species *i*
$c_{i,s}$ Surface molar concentration of species *i*
C_p Heat capacity at constant pressure
d Characteristic dimension
D_i Diffusion coefficientsta of species *i*
D_t Turbulent diffusion coefficient
e^- Electron
E Potential
E_b Passivity breakdown potential
E_{corr} Corrosion potential
E_{crit} Critical potential for localized corrosion
E_{rp} Repassivation potential
E_0 Equilibrium potential
f Friction factor
f_i Fugacity of species *i*
F Faraday constant
G^{ex} Excess Gibbs energy
i Current density
i_a Anodic current density
$i_{a,ct}$ Charge-transfer contribution to the anodic current density
$i_{a,L}$ Limiting anodic current density
i_c Cathodic current density
$i_{c,ct}$ Charge-transfer contribution to the cathodic current density
$i_{c,L}$ Limiting cathodic current density
i_{corr} Corrosion current density
i_p Passive current density
i_{rp} Current density limit for measuring repassivation potential
i_0 Exchange current density
i^* Concentration-independent coefficient in expressions for exchange current density
J_i Flux of species *i*
k_{ads} Adsorption rate constant
k_{des} Desorption rate constant
k_i Reaction rate constant for reaction *i*
$k_{m,i}$ Mass transfer coefficient for species *i*
K Equilibrium constant
K_{ads} Adsorption equilibrium constant
K_{sp} Solubility product
l_i Reaction rate for *i*th reaction
m_i Molality of species *i*
m_0 Standard molality of species *i*
n_i Number of moles of species or electrons
Nu Nusselt number
Pr Prandtl number
R Gas constant
R_k Rate of production or depletion of species *k*
Re Reynolds number
S Supersaturation
Sc Schmidt number
Sh Sherwood number
t Time
T Temperature
u_i Mobility of species *i*
v_i Rate of reaction *i*
V Linear velocity
z Direction perpendicular to the surface
z_i Charge of species *i*
α Thermal diffusivity
α_i Electrochemical transfer coefficient for species *i*
β Tafel coefficient using natural logarithms
γ_i Activity coefficient of species *i*
δ_i Nernst layer thickness for species *i*
$\Delta G_{ads,i}$ Gibbs energy of adsorption for species *i*
$\Delta H^{\neq}$ Enthalpy of activation
$\Delta\Phi$ Potential drop
ϵ Dielectric permittivity
η Dynamic viscosity
θ_i Coverage fraction of species *i*
θ_P Coverage fraction of passive layer
λ Thermal conductivity
μ_i Chemical potential of species *i*
μ_i^0 Standard chemical potential
$\bar{\mu}_i$ Electrochemical potential of species *i*
ν Kinematic viscosity
ν_i Stoichiometric coefficient of species *i*
ρ Density
Φ Electrical potential
ξ_i Electrochemical transfer coefficient for reaction *i*
ω Rotation rate
∇ Vector differential operator
$\equiv$**X** Surface species *X*

2.38.1 Introduction

Aqueous corrosion is an extremely complex physical phenomenon that depends on a multitude of factors including the metallurgy of the corroding metal, the chemistry of the corrosion-inducing aqueous phase, the presence of other – solid, gaseous, or nonaqueous liquid – phases, environmental constraints such as temperature and pressure, fluid flow characteristics, methods of fabrication, geometrical factors, and construction features. This inherent complexity makes the development of realistic physical models very challenging and, at the same time, provides a strong incentive for the development of practical models to understand the corrosion phenomena, and to assist in their mitigation. The need for tools for simulating aqueous corrosion has been recognized in various industries including oil and gas production and

transmission, oil refining, nuclear and fossil power generation, chemical processing, infrastructure maintenance, hazardous waste management, and so on. The past three decades have witnessed the development of increasingly sophisticated modeling tools, which has been made possible by the synergistic combination of improved understanding of corrosion mechanisms and rapid evolution of computational tools.

Corrosion modeling is an interdisciplinary undertaking that requires input from electrolyte thermodynamics, surface electrochemistry, fluid flow and mass transport modeling, and metallurgy. In this chapter, we put particular emphasis on corrosion chemistry by focusing on modeling both the bulk environment and the reactions at the corroding interface. The models that are reviewed in this chapter are intended to answer the following questions:

1. What are the aqueous and solid species that give rise to corrosion in a particular system? What are their thermophysical properties, and what phase behavior can be expected in the system? These questions can be answered by thermodynamic models.
2. What are the reactions that are responsible for corrosion at the interface? How are they influenced by the bulk solution chemistry and by flow conditions? How can passivity and formation of solid corrosion products be related to environmental conditions? How can the interfacial phenomena be related to observable corrosion rates? These questions belong to the realm of electrochemical kinetics and mass transport models.
3. What conditions need to be satisfied for the initiation and long-term occurrence of localized corrosion? This question can be answered by electrochemical models of localized corrosion.

These models can be further used as a foundation for larger-scale models for the spatial and temporal evolution of systems and engineering structures subject to localized and general corrosion. Also, they can be combined with probabilistic and expert system-type models of corrosion. Models of such kinds are, however, outside the scope of this review, and will be discussed in companion chapters.

2.38.2 Thermodynamic Modeling of Aqueous Corrosion

Historically, the first comprehensive approach to modeling aqueous corrosion was introduced by Pourbaix in the 1950s and 1960s on the basis of purely thermodynamic considerations.[1] Pourbaix[1] developed the *E*–pH stability diagrams, which indicate which phases are stable on a two-dimensional plane as a function of the potential and pH. The potential and pH were originally selected because they play a key role as independent variables in electrochemical corrosion. Just as importantly, they made it possible to construct the stability diagrams in a semianalytical way, which was crucial before the advent of computer calculations. Over the past four decades, great progress has been achieved in the thermodynamics of electrolyte systems, in particular for concentrated, mixed-solvent, and high temperature systems. These advances made it possible to improve the accuracy of the stability diagrams and, at the same time, increased the flexibility of thermodynamic analysis so that it can go well beyond the *E*–pH plane.

The basic objective of the thermodynamics of corrosion is to predict the conditions at which a given metal may react with a given environment, leading to the formation of dissolved ions or solid reaction products. Thermodynamics can predict the properties of the system in equilibrium or, if equilibrium is not achieved, it can predict the direction in which the system will move towards an equilibrium state. Thermodynamics does not provide any information on how rapidly the system will approach equilibrium, and, therefore, it cannot give the rate of corrosion.

The general condition of thermodynamic equilibrium is the equality of the electrochemical potential, $\bar{\mu}_i$ in coexisting phases,[2] that is,

$$\bar{\mu}_i = \mu_i + z_i F\phi = \mu_i^0 + RT \ln a_i + z_i F\phi \qquad [1]$$

where μ_i is the chemical potential of species i; μ_i^0, its standard chemical potential; a_i, the activity of the species; z_i, its charge; F, the Faraday constant; and ϕ is the electrical potential. The standard chemical potential is a function of the temperature and, secondarily, pressure. The activity depends on the temperature and solution composition and, to a lesser extent, on pressure. The activity is typically defined in terms of solution molality m_i,

$$a_i = (m_i/m^0)\gamma_i \qquad [2]$$

where m^0 is the standard molality unit (1 mol kg^{-1} H_2O), and γ_i is the activity coefficient. It should be noted that the molality basis for species activity becomes inconvenient for concentrated solutions because molality diverges to infinity as the concentration increases to the pure solute limit. Therefore, the mole fraction basis is more generally applicable for calculating activities.[3] Nevertheless, molality remains the most common concentration unit for aqueous systems and is used here for illustrative purposes.

Computation of μ_i^0 and γ_i is the central subject in electrolyte thermodynamics. Numerous methods, with various ranges of applicability, have been developed over the past several decades for their computation. Several comprehensive reviews of the available models are available (Zemaitis *et al.*,[4] Renon,[5] Pitzer,[6] Rafal *et al.*,[7] Loehe and Donohue,[8] Anderko *et al.*[3]). In the next section, the current status of modeling μ_i^0 and γ_i is outlined as it applies to the thermodynamics of corrosion.

2.38.2.1 Computation of Standard-State Chemical Potentials

The computation of the standard chemical potential μ_i^0 requires the knowledge of thermochemical data including

1. Gibbs energy of formation of species *i* at reference conditions (298.15 K and 1 bar).
2. Entropy or, alternatively, enthalpy of formation at reference conditions.
3. Heat capacity and volume as a function of temperature and pressure.

For numerous species, these values are available in various compilations (Chase *et al.*,[9] Barin and Platzki,[10] Cox *et al.*,[11] Glushko *et al.*,[12] Gurvich *et al.*,[13] Kelly,[14] Robie *et al.*,[15] Shock and Helgeson,[16] Shock *et al.*,[17,18] Stull *et al.*,[19] Wagman *et al.*,[20] and others). In general, thermochemical data are most abundant at near-ambient conditions, and their availability becomes more limited at elevated temperatures.

In the case of individual solid species, the chemical potential can be computed directly from tabulated thermochemical properties according to the standard thermodynamics.[2] In the case of ions and aqueous neutral species, the thermochemical properties listed above are standard partial molar properties rather than the properties of pure components. The standard partial molar properties are defined at infinite dilution in water. The temperature and pressure dependence of the partial molar heat capacity and the volume of ions and neutral aqueous species are quite complex because they are manifestations of the solvation of species, which is influenced by electrostatic and structural factors. Therefore, the computation of these quantities requires a realistic physical model.

An early approach to calculating the chemical potential of aqueous species as a function of temperature is the entropy correspondence principle of Criss and Cobble.[21] In this approach, heat capacities of various types of ions were correlated with the reference-state entropies of ions, thus making it possible to predict the temperature dependence of the standard chemical potential.

A comprehensive methodology for calculating the standard chemical potential was developed by Helgeson *et al.* (Helgeson *et al.*,[22] Tanger and Helgeson[23]). This methodology is based on a semi-empirical treatment of ion solvation, and results in an equation of state for the temperature and pressure dependence of the standard molal heat capacities and volumes. Subsequently, the heat capacities and volumes are used to arrive at a comprehensive equation of state for standard molal Gibbs energy and, hence, the standard chemical potential. The method is referred to as the HKF (Helgeson–Kirkham–Flowers) equation of state. An important advantage of the HKF equation is the availability of its parameters for a large number of ionic and neutral species (Shock and Helgeson,[16] Shock *et al.*,[18] Sverjensky *et al.*[24]). Also, correlations exist for the estimation of the parameters for species for which little experimental information is available. The HKF equation of state has been implemented both in publicly available codes (Johnson *et al.*[25]) and in commercial programs. A different equation of state for standard-state properties has been developed on the basis of fluctuation solution theory (Sedlbauer *et al.*,[26] Sedlbauer and Majer[27]). This equation offers improvement over HKF for nonionic solutes and in the near-critical region. However, the HKF remains as the most widely accepted model for ionic solutes.

2.38.2.2 Computation of Activity Coefficients

In real solutions, the activity coefficients of species deviate from unity because of a variety of ionic interaction phenomena, including long-range Coulombic interactions, specific ion–ion interactions, solvation phenomena, and short-range interactions between uncharged and charged species. Therefore, a practically-oriented activity coefficient model must represent a certain compromise between physical reality and computational expediency.

The treatment of solution chemistry is a particularly important feature of an electrolyte model. Here, the term 'solution chemistry' encompasses ionic dissociation, ion pair formation, hydrolysis of metal ions, formation of metal–ligand complexes, acid–base reactions, and so on. The available electrolyte models can be grouped in three classes:

1. models that treat electrolytes on an undissociated basis,
2. models that assume complete dissociation of all electrolytes into constituent ions, and

3. speciation-based models, which explicitly treat the solution chemistry.

The models that treat electrolytes as undissociated components are analogous to nonelectrolyte mixture models. They are particularly suitable for supercritical and high temperature systems, in which ion pairs predominate. Although this approach may also be used for phase equilibrium computations at moderate conditions (e.g., Kolker *et al.*[28]), it is not suitable for corrosion modeling because it ignores the existence of ions. The models that assume complete dissociation are the largest class of models for electrolytes at typical conditions. Compared with the models that treat electrolytes as undissociated or completely dissociated, the speciation-based models are more computationally demanding because of the need to solve multiple reactions and phase equilibria. Another fundamental difficulty associated with the use of speciation models lies in the need to define and characterize the species that are likely to exist in the system. In many cases, individual species can be clearly defined and experimentally verified in relatively dilute solutions. At high concentrations, the chemical identity of individual species (e.g., ion pairs or complexes) becomes ambiguous because a given ion has multiple neighbors of opposite sign, and, thus, many species lose their distinct chemical character. Therefore, the application of speciation models to concentrated solutions requires a careful analysis to separate the chemical effects from physical nonideality effects.

It should be noted that, as long as only phase equilibrium computations are of interest, comparable results could be obtained with models that belong to various classes. For example, the overall activity coefficients and vapor–liquid equilibria of many transition metal halide solutions, which show appreciable complexation, can be reasonably reproduced using Pitzer's[29] ion-interaction approach without taking speciation into account. However, it is important to include speciation effects for modeling the thermodynamics of aqueous corrosion. This is due to the fact that the presence of individual hydrolyzed forms, aqueous complexes, and so on is often crucial for the dissolution of metals and metal oxides. It should be noted that activity coefficients of individual species are different in fully speciated models than in models that treat speciation in a simplified way. Therefore, it is important to use activity coefficients that have been determined in a fully consistent way, that is, by assuming the appropriate chemical species in the solution.

The theory of liquid-phase nonideality is well-established for dilute solutions. A limiting law for activity coefficients was developed by Debye and Hückel[30] by considering the long-range electrostatic interactions of ions in a dielectric continuum. The Debye–Hückel theory predicts the activity coefficients as a function of the ionic charge and dielectric constant and density of the solvent. It reflects only electrostatic effects and, therefore, excludes all specific ionic interactions. Therefore, its range of applicability is limited to $\sim$0.01 M for typical systems. Several modifications of the Debye–Hückel theory have been proposed over the past several decades. The most successful modification was developed by Pitzer[29] who considered hard-core effects on electrostatic interactions. A more comprehensive treatment of the long-range electrostatic interactions can be obtained from the mean-spherical approximation (MSA) theory,[31,32] which provides a semianalytical solution for ions of different sizes in a dielectric continuum. The MSA theory results in a better prediction of the long-range contribution to activity coefficients at somewhat higher electrolyte concentrations.

The long-range electrostatic term provides a baseline for constructing models that are valid for electrolytes at concentrations that are important in practice. In most practically-oriented electrolyte models, the solution nonideality is defined by the excess Gibbs energy G^{ex}. The excess Gibbs energy is calculated as a sum of the long-range term and one or more terms that represent ion–ion, ion–molecule, and molecule–molecule interactions:

$$G^{ex} = G^{ex}_{long\text{-}range} + G^{ex}_{specific} + \cdots \qquad [3]$$

where the long-range contribution is usually calculated either from the Debye–Hückel or the MSA theory, and the specific interaction term(s) represent(s) all other interactions in an electrolyte solution. Subsequently, the activity coefficients are calculated according to standard thermodynamics[2] as

$$\ln \gamma_i = \frac{1}{RT}\left(\frac{\partial G^{ex}}{\partial n_i}\right)_{T,P,n_{j\neq i}} \qquad [4]$$

Table 1 lists a number of activity coefficient models that have been proposed in the literature, and shows the nature of the specific interaction terms that have been adopted. In general, these models can be subdivided into two classes:

1. models for aqueous systems; in special cases, such models can also be used for other solvents as long as the system contains a single solvent;
2. mixed-solvent electrolyte models, which allow multiple solvents as well as multiple solutes.

The aqueous electrolyte models incorporate various ion interaction terms, which are usually defined

Table 1 Summary of representative models for calculating activity coefficients in electrolyte systems

Reference	*Terms*	*Features*
Aqueous (or single-solvent) electrolyte models		
Debye and Hückel[30]	Long-range	Limiting law valid for very dilute solutions
Guggenheim[33,34]	Long-range + ion interaction	Simple ion interaction term to extend the Debye–Hückel limiting law; applicable to fairly dilute solutions
Helgeson[35]	Long-range + ion interaction	Ion interaction term to extend the limiting law; applicable to fairly dilute solutions
Pitzer[29]	Long-range + ion interaction	Ionic strength-dependent virial coefficient-type ion interaction term; revised Debye–Hückel limiting law; applicable to moderately concentrated solutions (~6 m)
Bromley[36]	Long range + ion interaction	Ionic strength dependent ion interaction term; applicable to moderately concentrated solutions (~6 m)
Zemaitis[37]	Long-range + ion interaction	Modification of the model of Bromley[36] to increase applicability range with respect to ionic strength
Meissner[38]	One-parameter correlation as a function of ionic strength	Generalized correlation to calculate activities based on a limited amount of experimental information
Pitzer and Simonson,[39] Clegg and Pitzer[40]	Long-range + ion interaction	Mole fraction-based expansion used for the ion interaction term; applicable to concentrated systems up to the fused salt limit
Mixed-solvent electrolyte models		
Chen *et al*.[41]	Long-range + short-range	Local-composition (NRTL) short-range term
Liu and Watanasiri[42]	Long-range + short-range + electrostatic solvation (Born) + ion interaction	Modification of the model of Chen *et al*.[41] using a Guggenheim-type ion interaction term for systems with two liquid phases
Abovsky *et al*.[43]	Long-range + short-range	Modification of the model of Chen *et al*.[41] using concentration-dependent NRTL parameters to extend applicability range with respect to electrolyte concentration
Chen *et al*.[44]	Long-range + short-range + ion hydration	Modification of the model of Chen *et al*.[41] using an analytical ion hydration term to extend applicability with respect to electrolyte concentration
Chen and Song[45]	Long-range + short-range + electrostatic solvation (Born)	Modification of the model of Chen *et al*.[41] by introducing segment interactions for organic molecules
Sander *et al*.[46]	Long-range + short-range	Local composition model (UNIQUAC) with concentration-dependent parameters used for short-range term
Macedo *et al*.[47]	Long-range + short-range	Local composition model (UNIQUAC) with concentration-dependent parameters used for short-range term
Kikic *et al*.[48]	Long-range + short range	Local composition group contribution model (UNIFAC) used for short-range term
Dahl and Macedo[49]	Short-range	Undissociated basis; no long-range contribution; group contribution model (UNIFAC) used for short-range term
Iliuta *et al*.[50]	Long-range + short-range	Local composition (UNIQUAC) model used for short-range term
Wu and Lee[31]	Extended long-range (MSA)	Mean-spherical approximation (MSA) theory used for the long-range term
Li *et al*.[51]	Long range + ion interaction + short range	Virial-type form used for the ion interaction term; local composition used for short-range term
Yan *et al*.[52]	Long-range + ion interaction + short range	Group contribution models used for both the ion interaction term and short-range term (UNIFAC)
Zerres and Prausnitz[53]	Long-range + short range + ion solvation	Van Laar model used for short-range term; stepwise ion solvation model
Kolker *et al*.[28]	Short-range	Undissociated basis; no long-range contribution
Wang *et al*.[54,55]	Long range + ion interaction + short range	Ionic strength-dependent virial expansion-type ion interaction term; local composition (UNIQUAC) short-range term; detailed treatment of solution chemistry
Papaiconomou *et al*.[32]	Extended long-range (MSA) + short-range	MSA theory used for the long-range term; local composition model (NRTL) used for the short-range term

in the form of virial-type expansions in terms of molality or mole fractions (see **Table 1**). Among these models, the Pitzer[29] molality-based model has found wide acceptance. Parameters of the Pitzer[29] model are available in the open literature for a large number of systems.[6]

The mixed-solvent electrolyte models are designed to handle a wider variety of chemistries. They invariably use the mole fraction and concentration scales. A common approach in the construction of mixed-solvent models is to use local-composition models for representing short-range interactions. The well-known local-composition models include NRTL, UNIQUAC, and its group-contribution version, UNIFAC (see Prausnitz *et al.*[56] and Malanowski and Anderko[57] for a review of these models). The local composition models are commonly used for nonelectrolyte mixtures and, therefore, it is natural to use them for short-range interactions in electrolyte systems. The combination of the long-range and local-composition terms is typically sufficient for representing the properties of moderately concentrated electrolytes in any combination of solvents. For systems that may reach very high concentrations with respect to electrolyte components (e.g., up to the fused salt limit), more complex approaches have been developed. One viable approach is to explicitly account for hydration and solvation equilibria in addition to using the long-range and short-range local composition terms (Zerres and Prausnitz,[53] Chen *et al.*[44]). A particularly effective approach is based on combining virial-type ion interaction terms with local composition models (Li *et al.*,[51] Yan *et al.*,[52] Wang *et al.*[54,55]). In such combined models, the local-composition term reflects the nonelectrolyte-like short-range interactions, whereas the virial-type ion interaction term represents primarily the specific ion–ion interactions that are not accounted for by the long-range contribution. These and other approaches are summarized in **Table 1**. Among the models summarized in **Table 1**, the models of Pitzer,[29] Zemaitis,[37] Chen *et al.*[41] (including their later modifications),[44,45] and Wang *et al.*[54,55] have been implemented in publicly available or commercial simulation programs.

2.38.2.3 Electrochemical Stability Diagrams

The *E*–pH diagrams, commonly referred to as the Pourbaix[1] diagrams, are historically the first, and remain the most important class of electrochemical stability diagrams. They were originally constructed for ideal solutions (i.e., on the assumption that $\gamma_i = 1$), which was the only viable approach at the time when they were introduced.[1] The essence of the procedure for generating the Pourbaix diagrams is analyzing all possible reactions between all – aqueous or solid – species that may exist in the system. The simultaneous analysis of the reactions makes it possible to determine the ranges of potential and pH at which a given species is stable. The reactions can be conveniently subdivided into two classes, that is, chemical and electrochemical reactions. The chemical reactions can be written without electrons, that is

$$\sum \nu_i M_i = 0 \qquad [5]$$

Then, the equilibrium condition for the reaction is given in terms of the chemical potentials of individual species by

$$\sum \nu_i \mu_i = 0 \qquad [6]$$

According to eqn [1], eqn [6] can be further rewritten in terms of species activities as

$$\sum \nu_i \ln a_i = -\frac{\sum \nu_i \mu_i^0}{RT} = \ln K \qquad [7]$$

where the right-hand side of eqn [7] is defined as the equilibrium constant because it does not depend on species concentrations.

In contrast to the chemical reactions, the electrochemical reactions involve electrons, e^-, as well as chemical substances M_i, that is

$$\sum \nu_i M_i + n e^- = 0 \qquad [8]$$

The equilibrium state of an electrochemical reaction is associated with a certain equilibrium potential. Since electrode potential cannot be measured on an absolute basis, it is necessary to choose an arbitrary scale against which the potentials can be calculated. If a reference electrode is selected, the equilibrium state of the reaction that takes place on the reference electrode is given by an equation analogous to eqn [8], that is

$$\sum \nu_{i,\mathrm{ref}} M_{i,\mathrm{ref}} + n e^- = 0 \qquad [9]$$

Then, the equilibrium potential E_0 of eqn [8] is given with respect to the reference electrode as

$$E_0 - E_{0,\mathrm{ref}} = \frac{\sum \nu_i \mu_i - \sum \nu_{I,\mathrm{ref}} \mu_{i,\mathrm{ref}}}{nF} \qquad [10]$$

According to a generally used convention, the standard hydrogen electrode (SHE) (i.e., $H^+(a_{H^+} = 1)/H_2(f_{H_2} = 1)$) is used as a reference. The corresponding reaction that takes place on the SHE is given by

$$H^+ - \frac{1}{2} H_2 + e^- = 0 \qquad [11]$$

Then, eqn [10] becomes

$$E_0 - E_{0,\text{ref}} = \frac{\sum \nu_i \mu_i - n\left(\mu^0_{H^+} - \frac{1}{2}\mu^0_{H_2}\right)}{nF} \quad [12]$$

In eqn [12], the standard chemical potentials μ^0_H and $\mu^0_{H_2}$ as well as the reference potential $E_{0,\text{ref}}$ are equal to zero at $T = 298.15$ K. For practical calculations at temperatures other than 298.15 K, two conventions can be used for the reference electrode. According to a universal convention established by the International Union of Pure and Applied Chemistry (the 'Stockholm convention'), the potential of SHE is arbitrarily defined as zero at all temperatures (i.e., $E_{0,\text{ref}} = 0$). When this convention is employed, eqn [12] is used as a working equation with $E_{0,\text{ref}} = 0$. In an alternate convention, the SHE reference potential is equal to zero only at room temperature, and its value at other temperatures depends on the actual, temperature-dependent values of $\mu^0_{H^+}$ and $\mu^0_{H_2}$. In this case, it is straightforward to show (see Chen and Aral,[58] Chen *et al.*,[59]) that eqn [12] becomes

$$E_0 = \frac{\sum \nu_i \mu_i}{nF} \quad [13]$$

at all temperatures. Equation [13] can be further rewritten in terms of activities as

$$E_0 = \frac{\sum \nu_i \mu^0_i}{nF} + \frac{RT}{nF}\sum \nu_i \ln a_i = E^0_0 + \frac{RT}{nF}\sum \nu_i \ln a_i \quad [14]$$

where E^0_0 is the standard equilibrium potential, which is calculated from the values of the standard chemical potentials μ^0_i.

For a brief outline of the essence of the Pourbaix diagrams, let us consider a generic reaction in which two species, A and B, undergo a transformation. The only other species that participate in the reaction are hydrogen ions and water, that is:

$$a\text{A} + c\text{H}_2\text{O} + n\text{e}^- = b\text{B} + m\text{H}^+ \quad [15]$$

If eqn [15] is a chemical reaction (i.e., if $n = 0$), then its equilibrium condition (eqn [7]) can be rewritten as

$$m\text{pH} = \log\left(\frac{a^a_B}{a^a_A}\right) - \log K - \log a^c_{H_2O} \quad [16]$$

where $\text{pH} = -\log a_{H^+}$, and decimal rather than natural logarithms is used. For dilute solutions, it is appropriate to assume that $a_{H_2O} = 1$, and the last term on the right-hand side of eqn [16] vanishes. If we assume that the components A and B are aqueous dissolved species and their activities are equal, eqn [16] defines the boundary between the predominance areas of species A and B. If one of the species (A or B) is a pure solid and the other is an aqueous species, the activity of the solid is equal to one and the activity of the aqueous species can be set equal to a certain predetermined, typically small, value (e.g., 10^{-6}). Then, eqn [16] represents the boundary between a solid and an aqueous species at a fixed value of the dissolved species activity. Similarly, for a boundary between two pure solid phases, the activities of the species A and B are equal to one. Such a boundary is represented by a vertical line in a potential–pH space, and its location depends on the equilibrium constant according to eqn [16].

If eqn [15] represents an electrochemical reaction (i.e., $n \neq 0$), the equilibrium condition (eqn [14]) becomes

$$E_0 = E^0_0 + \frac{RT}{nF}\ln\frac{a^a_A}{a^b_B} + \frac{RT}{nF}\ln a_{H_2O} + \frac{RT\ln 10}{F}\frac{m}{n}\text{pH} \quad [17]$$

As with the chemical reactions, the term that involves the activity of water vanishes for dilute solutions, and the ratio of the activities of species A and B can be fixed to represent the boundary between the predominance areas of two species. Under such assumptions, the plot of E versus pH is a straight line with a slope determined by the stoichiometric coefficients m and n.

Thus, for each species, boundaries can be established using eqns [16] and [17]. As long as the simplifying assumptions described above are met, the boundaries can be calculated analytically. By considering all possible boundaries, stability regions can be determined using an algorithm described by Pourbaix.[1] Sample E–pH diagrams are shown for iron in **Figure 1**.

One of the main reasons for the usefulness of stability diagrams is the fact that they can illustrate the interplay of various partial processes of oxidation and reduction. The classical E–pH diagrams contain two dashed lines, labeled as 'a' and 'b,' which are superimposed on the diagram of a given metal (see **Figure 1**). The dashed line 'a' represents the conditions of equilibrium between water (or hydrogen ions) and elemental hydrogen at unit hydrogen fugacity, that is

$$H^+ + e^- = 0.5H_2 \text{ (line 'a')} \quad [18]$$

The 'b' line describes the equilibrium between water and oxygen, also at unit fugacity,

$$O_2 + 4H^+ + 4e^- = 2H_2O \text{ (line 'b')} \quad [19]$$

Accordingly, water will be reduced to form hydrogen at potentials below line 'a,' and will be oxidized to form oxygen at potentials above line 'b.' The location

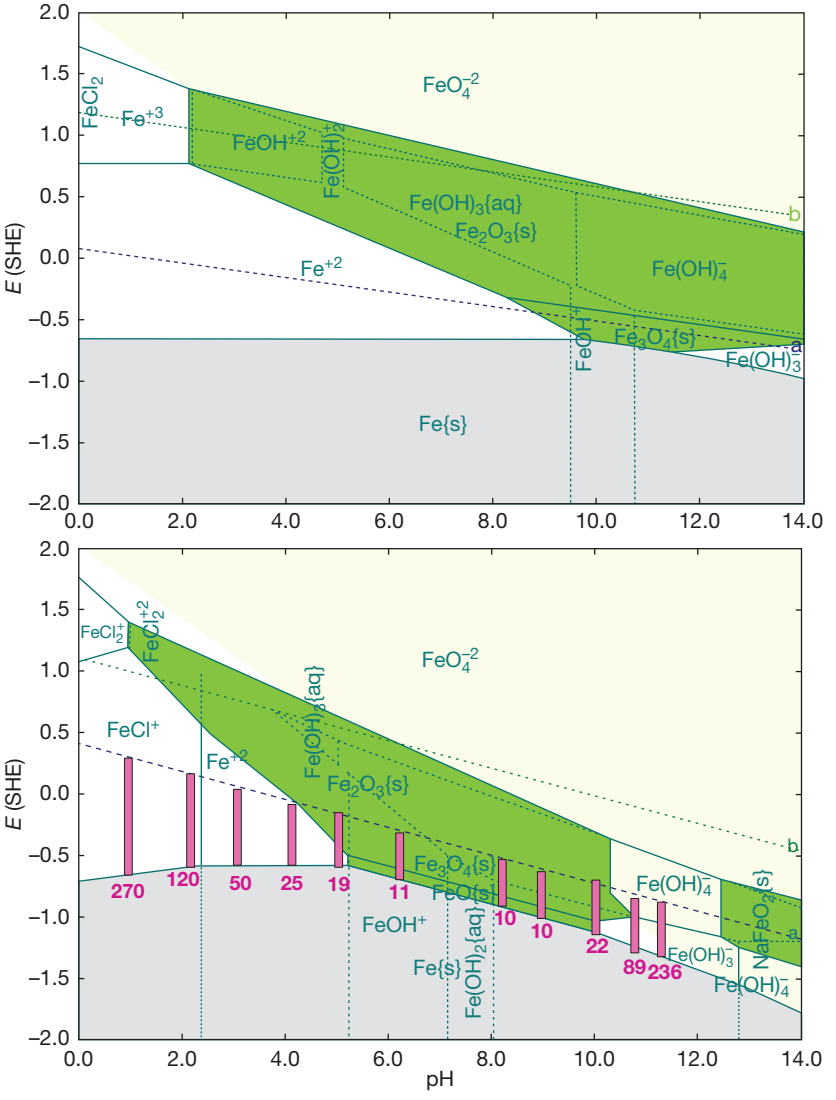

Figure 1 *E*–pH (Pourbaix) diagrams for iron at 25 °C (upper diagram) and 300 °C (lower diagram). At 300 °C, the conditions of the experiments of Partridge and Hall[60] are superimposed on the diagram. The vertical bars show the range between the equilibrium potentials for the reduction of H^+ and oxidation of Fe, thus bracketing the mixed potential in the experiments. The numbers under the bars denote the experimentally determined relative attack. The diagrams have been generated using the Corrosion Analyzer software[61] using the algorithm of Anderko *et al*.[62]

of the 'a' and 'b' lines on the diagram indicates whether a given redox couple is thermodynamically possible. For example, in the region between the line 'a' and the upper edge of the stability region of $Fe_{(s)}$ in **Figure 1**, the anodic reaction of iron oxidation can be coupled with the cathodic reaction of water or hydrogen ion reduction. In such a case, the measurable open-circuit potential of the corrosion process will establish itself between the line 'a' and the equilibrium potential for the oxidation of iron (i.e., the upper edge of the $Fe_{(s)}$ region). If the potential lies above line 'a,' then water reduction is no longer a viable cathodic process, and the oxidation of iron must be coupled with another reduction process. In the presence of oxygen, reaction eqn [19] can provide such a reaction process. In such a case, the open-circuit (corrosion) potential will establish itself at a higher value for which the upper limit will be defined by line 'b.'

Pourbaix[1] subdivided various regions of the *E*–pH diagrams into three categories, that is, immunity, corrosion, and passivation. The immunity region

encompasses the stability field of elemental metals. The corrosion region corresponds to the stability of dissolved, either ionic or neutral species. Finally, passivation denotes the region in which solid oxides or hydroxides are stable. In **Figure 1**, the immunity and passivation regions are shaded, whereas the corrosion region is not. It should be noted that this classification does not necessarily reflect the actual corrosion behavior of a metal. Only immunity has a strict significance in terms of thermodynamics because in this region the metal cannot corrode regardless of the time of exposure. The stability of dissolved species in the 'corrosion' region does not necessarily mean that the metal rapidly corrodes in this area. In reality, the rate of corrosion in this region may vary markedly because of kinetic reasons. Passivation is also an intrinsically kinetic phenomenon because the protectiveness of a solid layer on the surface of a metal is determined not by its low solubility alone. The presence of a sparingly soluble solid is typically a necessary, but not sufficient condition for passivity.

Although the *E*–pH diagrams indicate only the thermodynamic tendency for the stability of various metals, ions, and solid compounds, they may still provide useful qualitative clues as to the expected trends in corrosion rates. This is illustrated in the lower diagram of **Figure 1**. In this diagram, the vertical bars denote the difference between the equilibrium potentials for the reduction of water and oxidation of iron. Thus, the bars indicate the tendency of the metal to corrode in deaerated aqueous solutions with varying pH. They bracket the location of the corrosion potential and, thus, indicate whether the corrosion potential will establish itself in the 'corrosion' or 'passivation' regions. The numbers associated with the bars represent the experimentally determined relative attack. It is clear that the observed relative attack is substantially greater in the regions where a solid phase is predicted to be stable than in the regions where no solid phase is predicted. Thus, subject to the limitations discussed above, the stability diagrams can be used for the qualitative assessment of the tendency of metals to corrode, and for estimating the range of the corrosion potential.

Following the pioneering work of Pourbaix and his coworkers, further refinements of stability diagrams were made to extend their range of applicability. These refinements were made possible by the progress of the thermodynamics of electrolyte solutions and alloys. Specifically, further developments focused on

1. generation of diagrams at elevated temperatures,
2. taking into account the active solution species other than protons and water molecules,
3. introduction of solution nonideality, which influences the stability of species through realistically modeled activity coefficients,
4. introduction of alloying effects by accounting for the formation of mixed oxides and the nonideality of alloy components in the solid phase, and
5. flexible selection of independent variables, other than E and pH, for the generation of diagrams.

2.38.2.3.1 Diagrams at elevated temperatures

The key to the construction of stability diagrams at elevated temperatures is the calculation of the standard chemical potentials μ_i^0 of all individual species as a function of temperature. In earlier studies, the entropy correspondence principle of Criss and Cobble[21] was used for this purpose. Macdonald and Cragnolino[63] reviewed the development of *E*–pH diagrams at elevated temperatures until the late 1980s.

The HKF equation of state[22,23] formed a comprehensive basis for the development of *E*–pH diagrams at temperatures up to 300 °C for iron, zinc, chromium, nickel, copper, and other metals (Beverskog and Puigdomenech,[64–69] Anderko *et al.*[62]) An example of a high temperature *E*–pH diagram is shown for Fe at 300 °C in the lower diagram of **Figure 1**. Comparison of the Fe diagrams at room temperature and 300 °C shows a shift in the predominance domains of cations to lower pH values and an expansion of the domains of metal oxyanions at higher pH values. Such effects are relatively common for metal–water systems.

2.38.2.3.2 Effect of multiple active species

The concept of stability diagrams can be easily extended to solutions that contain multiple chemically active species other than H^+ and H_2O. In such a general case, the simple reaction eqn [15] needs to be extended as

$$v_X X + \sum_{i=1}^{k} v_i A_i = Y + v_e e^- \qquad [20]$$

where the species X and Y contain at least one common element and A_i ($i = 1, \ldots, k$) are the basis species that are necessary to define equilibrium equations between all species containing a given element. Reaction eqn [20] is normalized so that the stoichiometric coefficient for the right-hand side species (Y) is equal to 1. Such an extension results in generalized

expressions for the boundaries between predominance regions (eqns [16] and [17]). The equilibrium expression for the chemical reactions (eqn [20] with $v_e = 0$) then becomes

$$\ln K = \left(\ln a_Y - v_X \ln a_X - \sum_{i=1}^{k} v_i \ln a_{A_i} \right) = \frac{1}{RT} \left(\mu_Y^0 - \mu_X^0 - \sum_{i=1}^{k} v_i \mu_{A_i}^0 \right) \quad [21]$$

and the expression for an electrochemical reaction (eqn [20] with $v_e \neq 0$) takes the form:

$$E_0 = E_0^0 + \frac{RT}{Fv_e} \left(\ln a_Y - v_X \ln a_X - \sum_{i=1}^{k} v_i \ln a_{A_i} \right) \quad [22]$$

Thus, the expression for the boundary lines become more complicated but the algorithm for generating the diagrams remains the same, that is, the predominance areas can still be determined semianalytically.

The strongest effect of solution species on the stability diagrams of metals is observed in the case of complex-forming ligands and species that form stable, sparingly soluble solid phases other than oxides or hydroxides (e.g., sulfides or carbonates). Several authors focused on stability diagrams for metals such as iron, nickel, or copper in systems containing sulfur species (Biernat and Robbins,[70] Froning *et al.*,[71] Macdonald and Syrett,[72] Macdonald *et al.*,[73,74] Chen and Aral,[58] Chen *et al.*,[59] Anderko and Shuler[75]). This is due to the importance of iron sulfide phases, which have a strong tendency to form in aqueous environments even at very low concentrations of dissolved hydrogen sulfide. The stability domains of various iron sulfides can be clearly rationalized using *E*–pH diagrams. Diagrams have also been developed for metals in brines (Pourbaix,[76] Macdonald and Syrett,[72] Macdonald *et al.*,[73,74] Kesavan *et al.*,[77] Muñoz-Portero *et al.*[78]). The presence of halide ions manifests itself in the stability of various metal–halide complexes. Typically, the effect of halides on the thermodynamic stability is less pronounced than the effect of sulfides. However, concentrated brines can substantially shrink the stability regions of metal oxides and promote the active behavior of metals. An example of such effects is provided by the diagrams for copper in concentrated bromide brines (Muñoz-Portero *et al.*[78]) Effects of formation of various carbonate and sulfate phases have also been reported (Bianchi and Longhi,[79] Pourbaix[76]).

The formation of complexes of metal ions with organic ligands (e.g., chelants) frequently leads to a significant decrease in the stability of metal oxides, which may, under some conditions, indicate an increased dissolution tendency in the passive state (Silverman,[80,81] Kubal and Panacek,[82] Silverman and Silverman[83]). An important example of the importance of complexation is provided by the behavior of copper and other metals in ammoniated environments. **Figure 2** (upper diagram) illustrates an *E*–pH diagram for copper in a 0.2 m NH_3 solution. As shown in the figure, the copper oxide stability field is bisected by the stability area of an aqueous complex. The formation of a stable dissolved complex indicates that the passivity of copper and copper-base alloys may be adversely affected in weakly alkaline NH_3-containing environments. In reality, ammonia attack on copper-base alloys is observed in steam cycle environments.[63] Stability diagrams are a useful tool for the qualitative evaluation of the tendency of metals to corrode in such environments.

2.38.2.3.3 Diagrams for nonideal solutions

As long as the solution is assumed to be ideal (i.e., $\gamma_i = 1$ in eqn [2]), the chemical and electrochemical equilibrium expressions can be written in an analytical form, and the *E*–pH diagrams can be generated semianalytically. For nonideal solutions, the analytical character of the equilibrium lines can be preserved if fixed activity coefficients are assumed for each species (see Bianchi and Longhi[79]). However, such an approach does not have a general character because the activities of species change as a function of pH. This is due to the fact that, in real systems, pH changes result from varying concentrations of acids and bases, which influence the activity coefficients of all solution species. In a nonideal solution, the activities of all species are inextricably linked to each other because they all are obtained by differentiating the solution's excess Gibbs energy with respect to the number of moles of the individual species.[2] Therefore, in a general case, the equilibrium expressions (eqns [21] and [22]) can no longer be expressed by analytical expressions. This necessitates a modification of the algorithm for generating stability diagrams. A general methodology for constructing stability diagrams of nonideal solutions has been developed by Anderko *et al.*[62]

In general, the nonideality of aqueous solutions may shift the location of the equilibrium lines because the activity coefficients may vary by one or even two orders of magnitude. Such effects become pronounced in concentrated electrolyte solutions and in mixed-solvent solutions, in which water is not necessarily the predominant solvent.

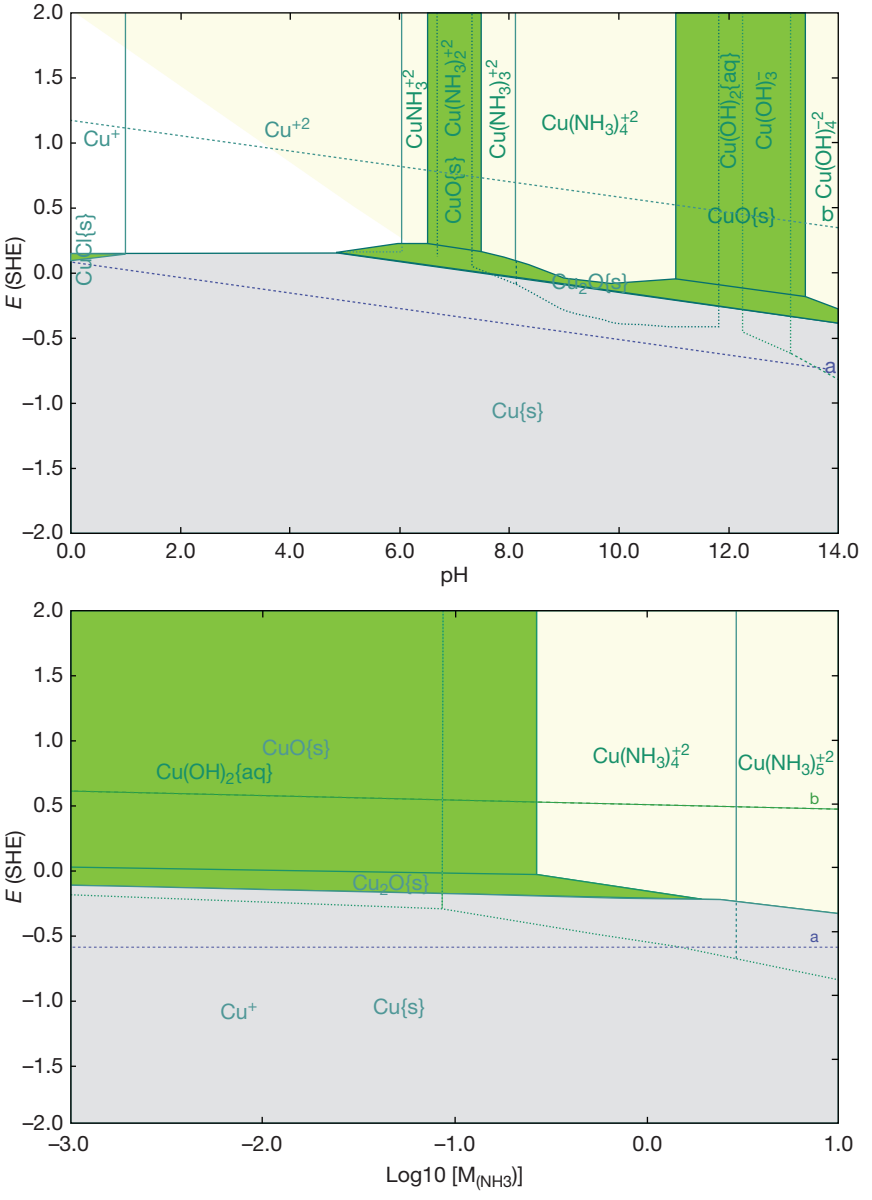

Figure 2 Use of thermodynamic stability diagrams to analyze the effect of ammonia on the corrosion of copper. The upper plot is an *E*–pH diagram for Cu in a 0.2 m NH_3 solution. The lower plot is a potential–ammonia molality diagram.

2.38.2.3.4 Diagrams for alloys

The vast majority of the published stability diagrams have been developed for pure metals. However, several studies have been devoted to generating stability diagrams for alloys, particularly those from the Fe–Ni–Cr–Mo family (Cubicciotti,[84,85] Beverskog and Puigdomenech,[69] Yang *et al.*,[86] Anderko *et al.*[87]). In general, a stability diagram for an alloy is a superposition of partial diagrams for the individual components of the alloy.[69] However, the partial diagrams are not independent because the alloy components form a solid solution and, therefore, their properties are linked. The superposition of partial diagrams makes it possible to analyze the tendency of alloy components for preferential dissolution. This may be the case when a diagram indicates that one alloy component has a tendency to form a passivating oxide, whereas another component has a tendency to form ions. Also, stability diagrams indicate in a simple way which alloy component is more anodic.